An Effective Pedestrian Dead Reckoning Algorithm Using a Unified Heading Error Model

Wei Chen[1, 2]
[1]Department of Electronic Science and Technology
University of Science and Technology of China (USTC)
Hefei, China
charlesw@mail.ustc.edu.cn

Ruizhi Chen[2], Yuwei Chen[2], Heidi Kuusniemi[2]
[2]Department of Navigation and Positioning
Finnish Geodetic Institute (FGI)
Masala, Finland

Jianyu Wang[3]
[3]Shanghai Institute of Technical Physics
Chinese Academy of Sciences
Shanghai, China

***Abstract*—Nowadays, navigation is an important application in mobile phones. However, locating a mobile user anytime anywhere is still a demanding task, because the GPS signal is easily corrupted or unavailable in urban canyons and indoor environments. Integrating GPS and self-contained dead reckoning sensors is an autonomous method to obtain a seamless positioning solution by means of Pedestrian Dead Reckoning (PDR) algorithms. A low-cost Multi-Sensor Positioning (MSP) platform has been developed by the Finnish Geodetic Institute, which includes a GPS receiver, a 2-axis digital compass and a 3-axis accelerometer. To construct a trajectory in GPS degraded environments, step length and the heading of each step are two key issues in PDR. In this paper, three typical estimation models of step length are presented and compared to demonstrate that in most cases, step length is not as critical as the determination of heading. Therefore, a unified heading error model is proposed, which includes all predictable errors from the navigation platform and the pedestrian's walking behavior, and applies to calibrating 2-axis magnetic compasses without tedious and complicated calibration procedures. Then the corresponding PDR algorithm is introduced, which integrates the step length estimated from a nonlinear model and the heading compensated by the unified model suggested through an Extended Kalman Filter (EKF). Several tests were conducted to validate the effectiveness of the heading error model and evaluate the positioning performance of this PDR algorithm. The results demonstrated that the heading error model is applicable for calibrating the 2-axis compass, and based on the PDR algorithm, the typical positioning performance of MSP can reach an accuracy of below 1.5% of the travelled distance during 10 minutes of continuous walking when GPS outages occur.**

Keywords-pedestrian dead reckoning; a unified heading error model; step length estimation; pedestrian navigation systems

I. INTRODUCTION

In pedestrian navigation, GPS is the primary means for providing accurate absolute position information. However, when a pedestrian walks in urban canyons or indoor environments, the positioning solutions are always corrupted or unavailable due to signal attenuation, interference, or blockage, etc. Therefore, it's essential to combine other navigation methods, such as dead reckoning (DR) sensors, pseudolites, Wi-Fi, UWB, and RFID to obtain a seamless positioning result. Integrating GPS with self-contained DR sensors is very promising, especially in urban environments, without any requirement for extra infrastructure, or a fingerprint database [1-11].

Based on low-cost self-contained Pedestrian Navigation Systems (PNS), pedestrian dead reckoning (PDR), which takes advantage of human physiological characteristics, generally outperforms the traditional inertial integration mechanism. The PDR algorithm utilizes accelerometers to detect the step occurrence and to estimate the step length via several effective models. However, due to the drift error of inexpensive gyros and the vulnerability of magnetic compasses to several types of errors, it is still a challenge to obtain an accurate heading and achieve a satisfactory positioning accuracy. Although most of systems are mounted on the pedestrian's shoe to reduce the drift error of gyros, making use of a step's stance phase for the zero velocity update (ZUPT), the positioning accuracy can't still hold up for more than a few minutes.

Considering the constraints of low cost, small size, and light weight, the Finnish Geodetic Institute (FGI) has developed a PNS, called a Multi-Sensor Positioning (MSP) platform [1], which integrates a GPS receiver, a 2-axis digital compass and a 3-axis accelerometer, as shown in Fig. 1. The objective of this paper is to propose an effective PDR algorithm based on the MSP, in order to achieve a both accurate and efficient seamless positioning solution in an urban environment, in which generally there exists less magnetic disturbances than in indoor environments.

Therefore, the paper continues with an introduction of the system architecture. Several step detection methods and step length estimation models are reviewed, and three typical step length models are chosen to compare the positioning performance of PDR, to illustrate that based on our PNS, in most cases, step length is not as critical as the determination of heading. Then a unified heading error model is proposed,

W. Chen is a Ph.D student of USTC, and is visiting at FGI, sponsored by the China Scholarship Council.

which includes all the predictable errors on 2-axis magnetic compasses. To construct the PDR trajectory, an EKF Kalman filter is realized using the estimated step length and compensated heading of each step. Consequently, results from several field tests are demonstrated to validate the heading error model suggested and evaluate the positioning performance of the corresponding PDR algorithm. Conclusions and future work are presented in the end.

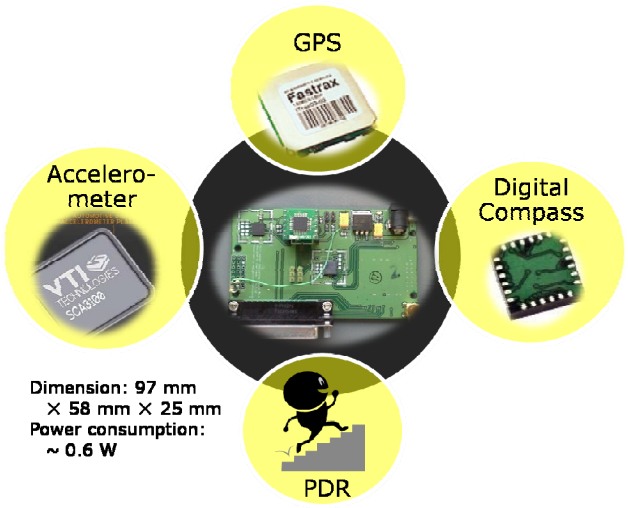

Figure 1. The hardware of the MSP

II. SYSTEM ARCHITECTURE

As shown in Fig. 1, the hardware of the MSP includes a Fastrax iTrax03 OEM GPS receiver with a positioning accuracy of about 2-5 m, a Honeywell 2-axis digital compass HMC6352 with a heading accuracy of about 2.5 degrees and a VTI 3-axis MEMS accelerometer SCA3000-D01 having a range of ±2 g. The receiver also includes a microprocessor which allows versatile programmability and can be used as a host controller [2]. Based on the MSP, to achieve a seamless positioning solution, the algorithm is designed as illustrated in Fig. 2. When the GPS signal is available, the final solution derives directly from the outputs of iTrax03 built-in Kalman filter. The speed and heading from GPS are utilized to train the step length model and calibrate the compass. When GPS outages occur, the PDR solution is adopted to bridge the gaps in a horizontal level, using the estimated step length and compensated heading from each model to propagate the pedestrian's position according to the following equation:

$$\begin{cases} E_{k+1} = E_k + l_k \cdot \sin a_k \\ N_{k+1} = N_k + l_k \cdot \cos a_k \end{cases}, \quad (1)$$

where E_k and N_k are the East and North coordinates, l_k is the step length and a_k is the heading at epoch k.

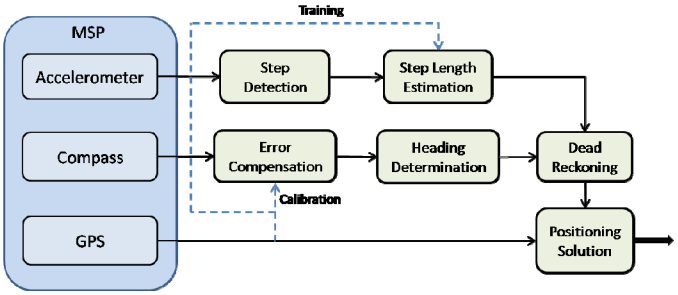

Figure 2. The PDR algorithm architecture of the MSP

III. STEP DETECTION AND STEP LENGTH ESTIMATION

In the traditional inertial integration mechanism, a pedestrian's speed and travelled distance could be derived via the integration of acceleration. To obtain an accurate acceleration, there are strict requirements of such as attitude alignment and high performance of accelerometers. However, due to the low-cost accelerometers in PNS, the positioning error is increased with the square of time, and complicated procedures such as attitude alignment and sensor calibration would ruin user experience in pedestrian navigation. Therefore, based on the fact that a pedestrian's gait is a cyclic pattern during walking and his/her step length shows good correlation with some statistical features of acceleration of each step, the PDR algorithm is utilized to detect the user's step, estimate the step length and calculate his/her travelled distance, avoiding the attitude alignment and the twice integral error with time.

To detect step occurrences, there are many effective methods, such as peak detection [3-5], zero-crossing [6], autocorrelation [7], stance-phase detection [8][9], FFT [3], and a method of adopting an impact switch mounted on the user's shoes to measure the steps directly [10]. In general, the accuracy of these methods can reach higher than 99%. The method adopted in this paper is a combination of three methods: sliding window, peak detection and zero-crossing, and can calculate the statistics of acceleration per step simultaneously [2].

Step length is determined according to different models that can be grouped into four categories: constant/quasi-constant model [8], linear model [3][4][6], nonlinear model [5], and Artificial Intelligence (AI) model [9][10][12]. Most of the models are established on a basis of good correlation between the walking speed and the statistical features of acceleration, such as step frequency, maximum or minimum value per step, variance per step, etc. Here are listed some typical models of the last three categories:

Linear model [4]:

$$SL = A + B \cdot SF + C \cdot SV, \quad (2)$$

where SL is step length, SF is step frequency and SV is the variance of acceleration of each step. A, B, C are the regressive parameters that can be determined in the training phase.

Nonlinear model [5]:

$$SL = K \cdot \sqrt[4]{A_{\max} - A_{\min}}\ , \tag{3}$$

where $A_{\max}$ (or $A_{\min}$) is the maximum (or minimum) acceleration at a step and K is the coefficient. In this model it is easy to implement real-time estimation algorithms due to only one parameter.

Artificial Neural Network (ANN) model: For the ANN approach, the main advantage is that we don't need to figure out an exact mapping relationship between step length and the statistic features of acceleration. The ANN model in this paper is a feed-forward back-propagation network that has a 16-node hidden layer with the 'tansig' transfer function. The nodes of the input layer in the model are fed by four parameters: SF, SV, $A_{\max}$ and $A_{\min}$.

To compare the performance of the three models presented above, a few tests have been conducted in open-sky environments. The testers walked along the track of a sports field, with the MSP and a Leica SR530 geodetic Real-Time Kinematic (RTK) receiver. Since the RTK receiver has a typical positioning accuracy of several centimeters under open-sky environments, the training and reference samples of step length are both derived from the RTK. Table I lists the results of step length estimation of the three models from one of these tests, and Fig. 3 illustrates the DR trajectories with the reference. Note that the trajectories based on the three models are constructed by the step length of each model and the reference heading from RTK according to (1), without regard to the error from heading. Furthermore, a DR trajectory is constructed using the reference step length and a heading from the digital compass of MSP that compensated the errors only from magnetic declination and hard-iron effect (the trajectory in cyan colour in Fig. 3). From these empirical results and some conclusions in the literature [5][8], we can learn that with respect to the error from heading, choosing different models of step length would not influence the positioning accuracy so severely. Therefore, in this paper, the nonlinear model (3) is chosen because of its one-parameter advantage.

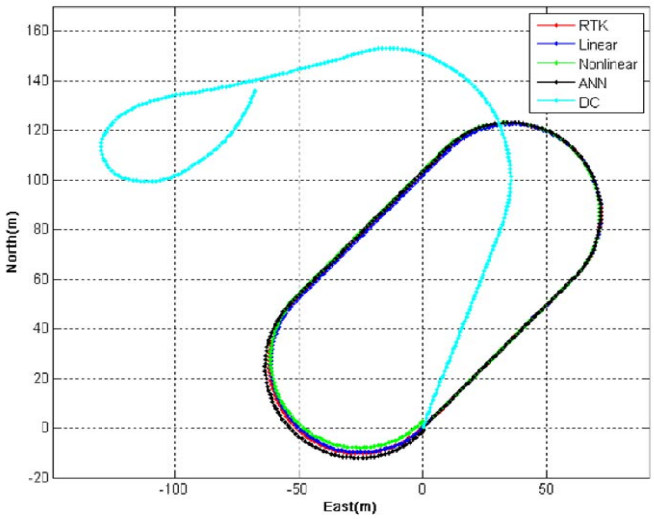

Figure 3. PDR results using three step length models

TABLE I. POSITIONING RESULTS OF THREE STEP LENGTH MODELS

Model	Linear	Nonlinear	ANN
Mean of step length error [m]	0.00	0.00	-0.01
Std of step length error [m]	0.04	0.04	0.05
Travelled distance error [%]	0.13	0.49	1.29
RMS of positioning error [m]	0.55	1.25	1.10
Max of positioning error [m]	1.29	2.35	1.93

IV. HEADING DETERMINATION

As discussed above, for achieving a practical PDR solution, it's essential to eliminate the errors of the 2- axis compass.

A magnetic compass measures the intensity of the Earth's magnetic field [13], and provides angle information with respect to magnetic north through the following equation [14]

$$H(M_x, M_y) = \arctan(-\frac{M_y}{M_x})\ , \tag{4}$$

where (M_x, M_y) are the magnetic readings in level plane.

However, the outputs of a magnetic compass are easily corrupted by several errors, which can be grouped into two categories: predictable errors from sources such as hard and soft iron effects, tilt of the platform, installation misalignment, and magnetic declination, as well as unpredictable errors mainly from environmental magnetic disturbances. Some predictable errors can be eliminated by a calibration procedure or a real-time compensation algorithm. The unpredictable errors are difficult to be removed, so that the heading in an indoor environment with severe magnetic disturbances is too poor to be used. This paper will focus on how to eliminate these predictable errors.

A. *Predictable Errors of the Magnetic Compass*

In a self-developed PNS, as shown below, there are usually several types of predictable errors of a 2-axis digital compass.

1) Magnetic declination: The difference from geographical north to magnetic north, denoted as λ.

2) Hard and soft iron effects from ferrous materials in the platform: The hard iron effect is always considered as biases of sensors' metrical axes, denoted as [14]

$$C_b = (C_{bx}, C_{by}, 0)^T\ , \tag{5}$$

The error from the soft iron effect is modeled as [14]

$$C_s = \begin{bmatrix} 1+a_{xx} & a_{xy} & a_{xz} \\ a_{yx} & 1+a_{yy} & a_{yz} \\ 0 & 0 & 1 \end{bmatrix}. \tag{6}$$

3) Scale factors and biases: Scale factors and drift-free biases of metrical axes can be grouped into soft iron and hard iron effects separately [15].

4) Tilt of the platform: A 2-axis digital compass should be confined in a horizontal plane, or the vertical component of the Earth's magnetic field will be projected on the two axes of the compass and cause a large error when the platform is tilted. The tilt error is given by a rotation matrix R_L^B from Local Level Frame (LLF) to the body frame

$$R_L^B = \begin{bmatrix} \cos\varphi & \sin\varphi\cdot\sin\theta & \sin\varphi\cdot\cos\theta \\ 0 & \cos\theta & -\sin\theta \\ -\sin\varphi & \cos\varphi\cdot\sin\theta & \cos\varphi\cdot\cos\theta \end{bmatrix}, \quad (7)$$

where φ is the pitch angle and θ is the roll angle.

5) Misalignment: The deviation between the forward direction of the body frame and the true heading the pedestrian walks. The misalignment is a constant and is denoted as β.

6) Oscillation of the pedestrian's body when walking: Due to the oscillation of the user's body when walking, the platform is vibrated accordingly. According to the empirical experience of the authors, the influence on the heading can be modeled as Gaussian noise $\omega \sim N(0, \sigma^2)$, where σ^2 is the variance of the heading and is decided by the walking speed. It's a unique error in pedestrian navigation rather than in vehicle navigation, and can cause a more severe fluctuation on the heading of 3-axis magnetic compasses than on the one of 2-axis compasses, because the pedestrian's acceleration from both the walking and the corresponding body oscillation would affect the outputs of the tilt sensor [16] and mess up the built-in tilt compensation algorithm. Fig. 4 shows this phenomenon between a standalone 3-axis compass module and the 2-axis compass of MSP, from a test that the user equipped with both devices walked along the track of a sports field two rounds.

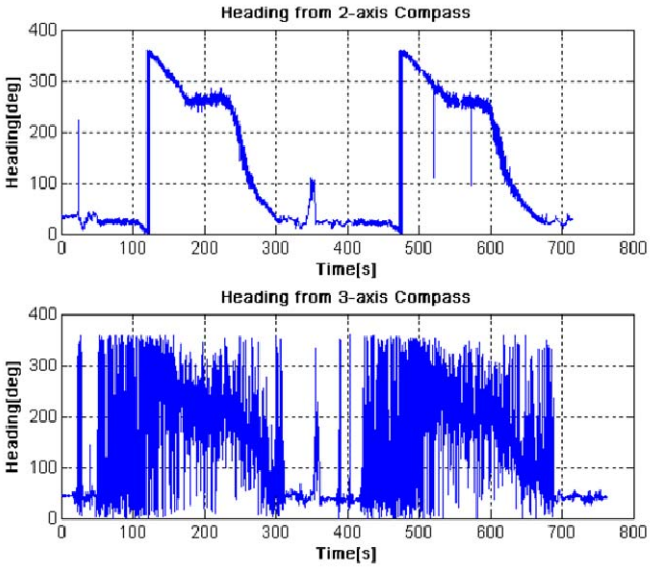

Figure 4. Raw heading from a 2-axis compass and a 3-axis compass

Many papers are addressed on diminishing these errors. In [13], a handy and popular method is provided to reduce the hard and soft iron effects in a vehicle, but can't completely get rid of the errors from the soft iron effect because of not considering the cross influence between two horizontal axes of the compass. For compensating the tilt of the platform, generally a 3-axis compass with a tilt sensor is necessary, as in [13-15]. In [9] and [17], although a tilt-compensating algorithm for a 2-axis compass applied in pedestrian navigation is proposed, it still needs an accelerometer as the tilt sensor and external information on the magnetic inclination. In addition, the compass must be mounted on the shoe and the errors are reduced during the stance phase of each step. A rigorous calibration approach in the magnetic field domain has been proposed in [14], and [15] introduces a similar method from the viewpoint of geometrics. A method in [18] is utilized to directly estimate the errors in the heading from the compass mounted on ships, except tilt compensation.

However, considering the requirements in pedestrian navigation, such as user experience, hardware limitation and computational efficiency of the error compensation algorithm, there is not a suitable approach to calibrate the 2-axis compass of MSP. Therefore, an adaptive calibration approach intended for a 2-axis compass applied in pedestrian navigation is proposed in the following section, based on a unified error model including all the predictable errors, without any hardware requirements of a 3-axis magnetometer and a tilt sensor, or algorithm requirements of massive computational resources, or the limitation on where the system should be placed. Besides, the presented approach combines static and dynamic calibrations into one calibration procedure in open-sky environments before continuous navigation, and is easy-to-use whenever required by the compass.

B. An Adaptive Calibration Approach using a Unified Error Model

According to the definition of these predictable errors, the actual measurement vector in the body frame, $M_b = (M_{bx}, M_{by}, M_{bz})^T$ is

$$M_b = R_L^B (C_s M_h + C_b), \quad (8)$$

where $M_h = (M_{hx}, M_{hy}, M_{hz})^T$ is the Earth's magnetic components. The true heading with respect to the north ξ is

$$\xi = H(M_{hx}, M_{hy}) + \lambda + \beta + \omega, \quad (9)$$

while the raw heading from the compass, ξ', is

$$\xi' = H(M_{bx}, M_{by}). \quad (10)$$

Therefore, the unified model including all the predictable errors can be expressed as follows:

$$\delta = \xi - \xi' = H(M_{hx}, M_{hy}) - H(M_{bx}, M_{by}) + \lambda + \beta + \omega, \quad (11)$$

where δ is the deviation between the true heading and the raw heading. Note that substituting (5) - (7) into (8) gives the same form with the equation in [18] (pp. 67-85), eventually the comprehensive error in (11) can be determined approximately via

$$\delta = A + B\sin(\xi') + C\cos(\xi') + D\sin(2\xi') + E\cos(2\xi') + \omega \,, \quad (12)$$

where A - E are determined in the calibration procedure.

As known from (12), if the raw headings from the compass and the corresponding reference heading from the GPS are obtained in the calibration procedure, which takes just one or two minutes in an open-sky environment, the parameters in (9) can be calculated by a least square method. After the procedure, the heading error can be estimated in real-time and the residual resulting mostly from the oscillation of the body can be reduced through a Kalman filter.

V. PEDESTRIAN DEAD RECKONING ALGORITHM

To construct the PDR trajectory, an Extended Kalman Filter (EKF) is realized to combine the prediction values and the measurements optimally. The state vector includes the four parameters in (1), that is $[E_k \;\; N_k \;\; l_k \;\; a_k]$, and the state equation is designed as follows, assuming the step length l_k and step heading a_k are both a random walk process:

$$\begin{cases} E_{k+1} = E_k + l_k \cdot \sin a_k \\ N_{k+1} = N_k + l_k \cdot \cos a_k \\ l_{k+1} = l_k + w_l \\ a_{k+1} = a_k + w_a \end{cases}, \quad (13)$$

where $w_l \sim \mathrm{N}(0, \delta_l^2)$ and $w_a \sim \mathrm{N}(0, \delta_a^2)$. The measurement vector includes the estimated step length and compensated heading at the current step. Since the state equation is not linear, it should be linearized and an EKF is finally involved in the PDR algorithm to get the most optimal estimate states, according to the principle of EKF introduced in [19].

VI. EXPERIMENTS AND RESULTS

To validate this calibration approach and evaluate the performance of the PDR algorithm based on the MSP, extensive field tests were conducted in different scenarios. As illustrated in Fig. 5, the MSP was strapped to the pedestrian's abdominal area, and the GPS antenna was fixed on top of a cap for maximum satellite visibility. The data were stored in a laptop during the test and post-processed later on.

A. Validation of The Heading Error Model

The first test was designed to verify whether the experimental errors in the heading without any calibration could be consistent with the theoretical result from (12), and whether the proposed model was suitable enough for representing the predictable errors of a 2-axis compass. Hence three pedestrians were asked to walk along a 400 m track for one round at different places. The heading from iTrax03 GPS was used to train the error model and as a reference. As shown in Fig. 6, four sets of heading error (in blue color) appear similarly in the waveform, all representing a sinusoid. After calculating the calibration parameters (listed in Table Ⅱ), the estimated error is shown in the same figure in parallel. The histogram of residuals is illustrated in Fig. 7. Respectively, 78%, 83%, 94% and 92% of the residuals in the four sets of data are in the range of [-5°, 5°], and the distribution characteristics basically coincide with the hypothesis that the error from the oscillation of the body can be feasibly modeled as Gaussian noise. Besides, note that in Table Ⅱ these values are unique at each test due to different tilts of platform and various magnetic environments when installing the system. The reason why the values in the first two data are remarkably larger than others is that, we mounted another two devices in the proximity of the MSP, which brought extra hard and soft iron errors on the compass. This phenomenon demonstrates that the adaptability of calibration approaches is essential to eliminate the fortuitously introduced but predictable errors.

These results indicate that it is applicable to utilize the proposed model for representing the predictable errors. Once the parameters are determined in the calibration procedure, for example, walking along a track for one round, the heading error during the navigation mission can be real-time eliminated.

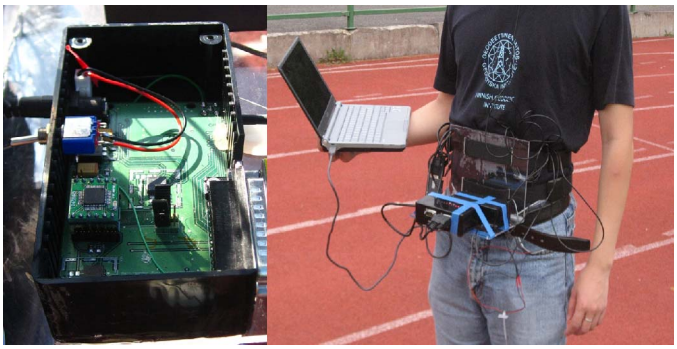

Figure 5. Placement of the MSP on the pedestrian's body

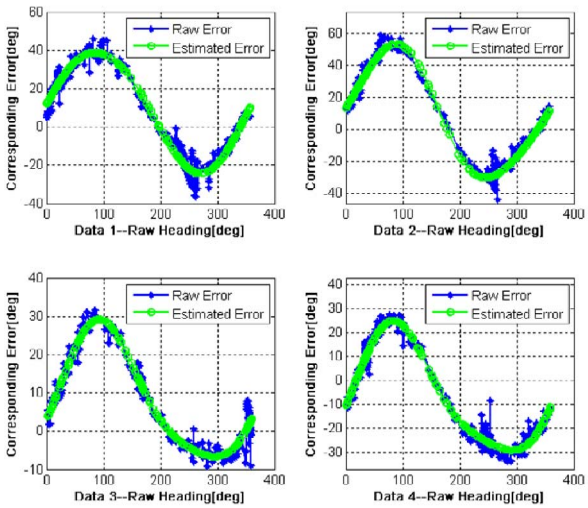

Figure 6. Raw heading error and estimated error

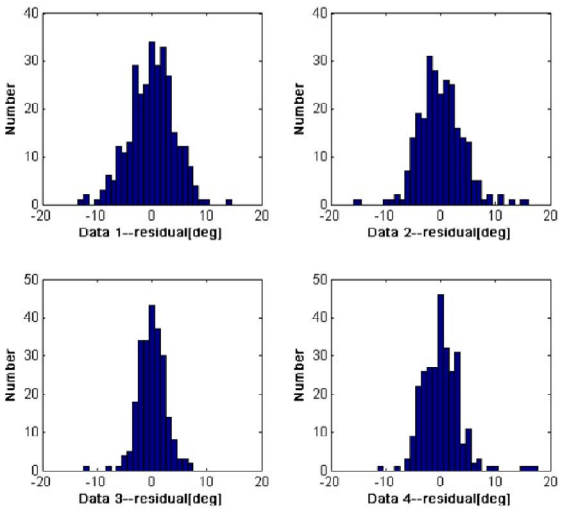

Figure 7. Distribution of the heading residuals

TABLE II. VALUES OF THE CALIBRATION PARAMETERS

Data	A[deg]	B[deg]	C[deg]	D[deg]	E[deg]
1	9.0	31.4	0.9	0.6	1.8
2	9.1	40.3	7.7	-3.1	-3.9
3	8.7	17.4	-2.3	0.6	-3.1
4	-6.2	26.3	0.1	2.6	-4.5

B. Evaluation of The PDR Algorithm

After validating the effectiveness of this calibration approach, we conducted two other tests at different places, took them as simulated GPS gaps and calculated the pure DR results of each test to evaluate the PDR performance based on the MSP. During each test, the tester first performed a calibration on the digital compass and trained the step length model in a sports field using the data from iTrax03 GPS, then got out of the sports field and walked along the prescribed trajectory as displayed in Fig. 8 separately. Besides the MSP, the tester also took a Leica SR530 geodetic RTK receiver for obtaining precise positioning reference. However, since its strict requirement of GPS signal visibility, the RTK receiver couldn't get a continuous positioning solution, when the tester was walking by the trees; while the iTrax03 GPS got the GPS solution through each test. Hence at each test, we evaluated the positioning accuracy of the PDR algorithm only at those points that the position coordinates from the RTK receiver are available, and used the step length and step heading interpolated from the outputs of the iTrax03 GPS built-in Kalman filter as reference samples to assess the performance of the heading error model and step length estimation model.

Fig. 9 presents the PDR trajectory of each test, separately in (a) and (b), as well as the discontinuous reference points from the RTK receiver and the continuous solution from iTrax03 GPS. The positioning performance is compared at those points having a RTK solution, and the corresponding positioning errors are shown both in Fig. 10 and Table Ⅲ. The positioning performance of the PDR algorithm in both tests in terms of RMS can achieve an accuracy of below 1.5% of the traveled distance during 10.5 minutes (6.5 minutes) of continuous walking. Furthermore, using the step length and step heading interpolated from the iTrax03 GPS as reference samples, the corresponding results from the heading error model and step length model are illustrated in Fig. 11 and Table Ⅳ. Although the position coordinates from iTrax03 GPS is quite good under these woody environments as demonstrated in Fig. 9, the speed from it is a little bit noisy in such environments. Nevertheless, comparison between the GPS-derived and PDR-derived step lengths can still reflect the effectiveness of the step length model. Besides, the heading residuals after being compensated by the unified error model suggested have been reduced to an acceptable level, of which the average is below 1 degree and the standard deviation is several degrees mostly due to the oscillation of the pedestrian's body. These results indicate that the proposed model can eliminate the predictable errors effectively and adaptively, especially compensating the tilt of the platform without the help of tilt sensors or external information on local magnetic field.

(a)

(b)

Figure 8. The nominal trajectories of the two tests: (a) in Kirkkonummi, Finland; (b) in Espoo, Finland

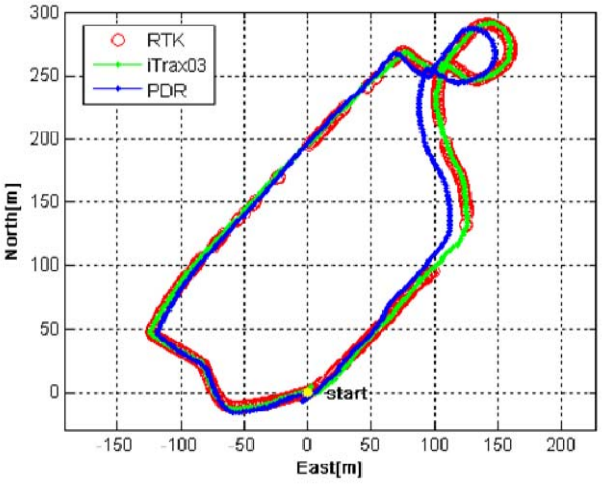

(a)

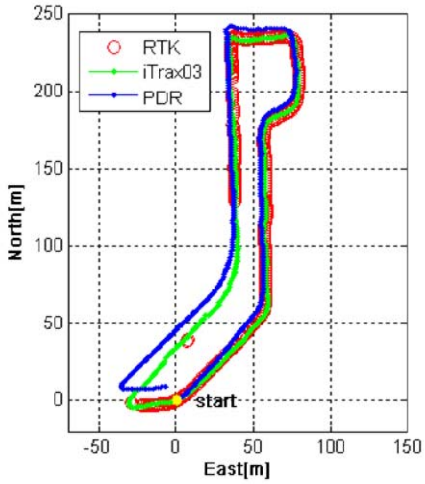

(b)

Figure 9. Positioning results of the two tests: (a) in Kirkkonummi, Finland; (b) in Espoo, Finland

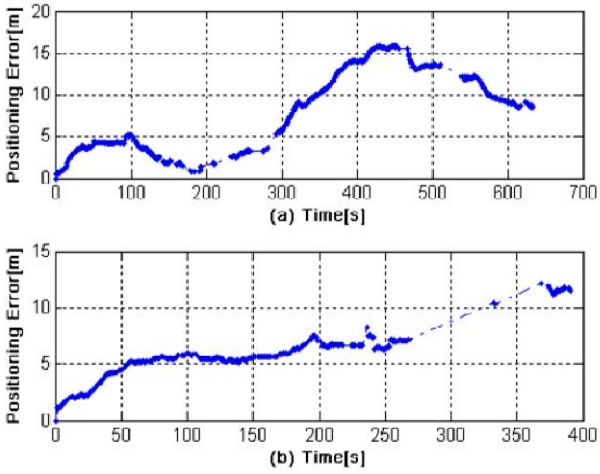

Figure 10. Positioning errors of the two tests: (a) in Kirkkonummi, Finland; (b) in Espoo, Finland

TABLE III. POSITIONING RESULTS OF THE TWO TESTS (RTK AS REFERENCE)

Test	Walk Time [s]	Travelled Distance from iTrax03 [m]	RMS [m]	RMS [%]	Max [m]	Max [%]
a	634	932.0	9.4	1.01	15.9	1.71
b	390	591.2	6.2	1.04	12.1	2.05

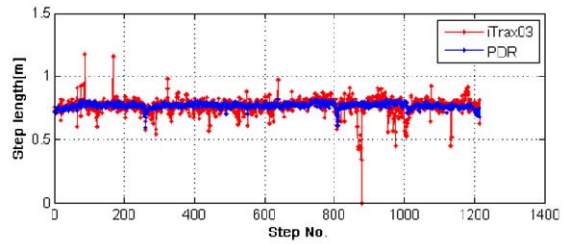

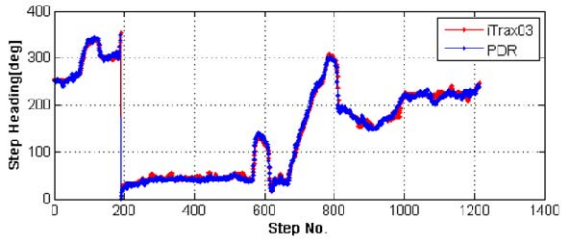

(a)

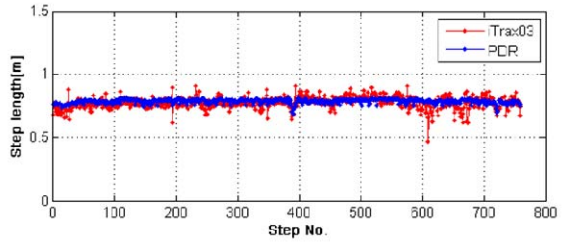

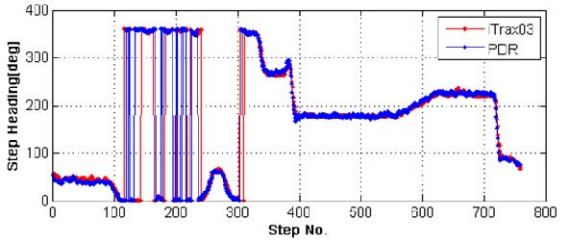

(b)

Figure 11. Step length and step heading comparison of the two tests: (a) in Kirkkonummi, Finland; (b) in Espoo, Finland

TABLE IV. STEP LENGTH AND STEP HEADING RESULTS OF THE TWO TESTS (iTrax03 AS REFERENCE)

Test	Step Length Error		Heading Error		Estimated Travelled Distance [m]	Travelled Distance Error [%]
	Mean [m]	Std [m]	Mean [deg]	Std [deg]		
a	-0.00	0.07	0.61	6.51	938.9	0.74
b	-0.01	0.04	0.60	5.05	602.3	1.88

VII. CONCLUSIONS AND FUTURE WORK

This paper introduces how to develop an effective PDR algorithm based on a low-cost self-developed PNS, including two key issues: step length estimation and determination of heading. Three typical models for estimating the step length are compared, for demonstrating that generally the step length is less important than the determination of heading in PDR. Therefore, a unified heading error model is proposed for calibrating 2-axis digital compasses applied in pedestrian navigation, including all the predictable errors from the navigation platform and the pedestrian's walking behavior. Several tests were conducted for validating the credibility of this heading error model and evaluating the positioning performance of the corresponding PDR algorithm. The results demonstrate that the heading error model is effective and the PDR algorithm proposed is applicable for the MSP.

However, a separate calibration procedure is more or less inconvenient for mobile pedestrian navigation applications. Future work is to realize a real-time training mechanism for the heading error model. Besides, the heading error model is targeted for eliminating only the predictable errors of magnetic compasses, and how to reduce the unpredictable errors and obtain an accurate heading in the environments with many magnetic disturbances is to be investigated next step.

REFERENCES

[1] R. Chen, Y. Chen, L. Pei, W. Chen, H. Kuusniemi, J. Liu, H. Leppäkoski, and J. Takala, "A DSP-based multi-sensor multi-network positioning platform," Proc. ION GNSS 2009, Savannah, Georgia, USA.

[2] W. Chen, Z. Fu, R. Chen, Y. Chen, O. Andrei, T. Kroger, and J. Wang, "An integrated GPS and multi-sensor pedestrian positioning system for 3D urban navigation," Proc. Urban Remote Sensing Event, 2009 Joint, Shanghai, China.

[3] R. Levi and T. Judd, "Dead reckoning navigational system using accelerometer to measure foot impacts," U. S. Patent US5583776.

[4] Q. Ladetto, "On foot navigation: continuous step calibration using both complementary recursive prediction and adaptive Kalman filtering," Proc. of ION GPS 2000, Salt Lake City, UT, USA.

[5] L. Fang, P. Antsaklis, L. Montestruque, M. McMickell, M. Lemmon,Y. Sun, H. Fang, I. Koutroulis, M. Haenggi, M. Xie, and X. Xie, "Design of a wireless assisted pedestrian dead reckoning system - the NavMote experience," IEEE Trans. Instrum. and Meas., vol. 54, no. 6, 2005, pp. 2342-2358.

[6] J. Käppi, J. Syrjärinne, and J. Saarinen, "MEMS-IMU based pedestrian navigator for handheld devices," Proc. of ION GPS 2001, Salt Lake City, UT, USA.

[7] F. Weimann and G. Abwerzger, "A pedestrian navigation system for urban and indoor environments," Proc. ION GNSS 20th International Technical Meeting, Fort Worth, TX, USA, 2007.

[8] G. Lachapelle, S. Godha and M. E. Cannon, "Performance of integrated HSGPS-IMU technology for pedestrian navigation under signal masking," Proc. European Navigation Conference, Manchester, UK, 2006.

[9] S. Cho and C. Park, "MEMS based pedestrian navigation system," The Journal of Navigation, vol. 59, pp. 135-153, 2006.

[10] D. A. Grejner-Brzezinska, C. K. Toth, and S. Moafipoor, "Pedestrian tracking and navigation using an adaptive knowledge system based on neural networks," Journal of Applied Geodesy, vol. 1, no.3, pp. 111-123, 2007.

[11] G. Retscher, "Test and integration of location sensors for a multi-sensor personal navigator," The Journal of Navigation, vol. 60, pp. 107-117, 2007.

[12] S. Moafipoor, D. A. Grejner-Brzezinska, and C. K. Toth, "A fuzzy dead reckoning algorithm for a personal navigator," Journal of The Institute of Navigation, vol. 55, No. 4, pp. 241-254, Winter 2008.

[13] M. J. Caruso, "Applications of magnetoresistive sensors in navigation systems," Sensors and Actuators, SAE SP-1220, pp. 15-21, 1997.

[14] D. Gebre-Egziabher, G. Elkaim, J. Powell, and B. Parkinson, "Calibration of strapdown magnetometers in magnetic field domain," ASCE Journal of Aerospace Engineering, vol. 19, no. 2, pp. 1-16, 2006.

[15] J. Vasconcelos, G. Elkaim, C. Silvestre, P. Oliveira and B. Cardeira, "A geometric approach to strapdown magnetometer calibration in sensor frame," Proc. IFAC Workshop on Navigation, Guidance, and Control of Underwater Vehicles (NGCUV), Killaloe, Ireland, April 2008.

[16] M. J. Caruso, "Applications of magnetic sensors for low cost compass systems," Proc. IEEE Position Location and Navigation Symposium (PLANS) 2000, San-Deigo, CA, USA.

[17] S. Cho and C. Park, "Tilt compemsation algorithm for 2-axis magnetic compass," IEEE Electronics Lett., vol. 39, no. 22, Oct. 2003.

[18] W. Denne, Magnetic Compass Deviation and Correction, Glasgow, Scotland: Brown, Son & Ferguson, Ltd., 1998.

[19] R. G. Brown and P. Y. C. Hwang, Introduction to Random Signals and Applied Kalman Filtering, 3rd ed., John Wiley & Sons, Inc., 1997.